Astrophys Space Sci (2013) 346:463–475
DOI 10.1007/s10509-013-1452-z

ORIGINAL ARTICLE

Discovery of a coherent oscillation with a 1.07 h period in the suspected cataclysmic variable FBS 1220 + 753 (Dra 7)

V.P. Kozhevnikov

Received: 20 December 2012 / Accepted: 9 April 2013 / Published online: 20 April 2013

Abstract We report results of extensive photometry of the suspected cataclysmic variable FBS 1220 + 753. The observations were obtained over 28 nights in 2010, 2011 and 2012. The total duration of the observations was 160 h. We clearly detected the highly coherent oscillation with a period of 1.0712887 ± 0.0000013 h and a stable semi-amplitude of 0.03 mag. In a time scale of years, the oscillation period is very stable ($dP/dt < (4.1 \pm 1.4) \times 10^{-10}$). The light curves of FBS 1220 + 753 show no obvious flickering. The significant brightness changes on large time intervals are also absent. Therefore, it is unlikely that FBS 1220 + 753 is a cataclysmic variable. The period is compatible with oscillations seen in δ Sct variables. But its high stability and the unchangeable oscillation amplitude suggest that the oscillation cannot be caused by multiperiodic stellar pulsations. The average pulse shape of the oscillation is very sinusoidal with slightly sharper maxima compared with minima, but it is somewhat changeable from year to year. The light curves obtained in 2011 and folded with the doubled oscillation period reveal that the adjacent oscillation cycles have slightly different depths of the minima and different steepness of the rise and decline. This behaviour resembles the behaviour of the binary subdwarf–white dwarf systems, in which the variability is caused by ellipsoidal variations. However, the folded light curve obtained from the data of 2010 reveal nearly equal shapes of the adjacent oscillation cycles, and this does not conform to such an interpretation. Thus, the nature of the oscillation seen in FBS 1220 + 753 remains puzzling. To solve this puzzle, detailed spectroscopic observations are needed.

V.P. Kozhevnikov (✉)
Astronomical Observatory, Ural Federal University, Lenin Av. 51, Ekaterinburg 620083, Russia
e-mail: valerij.kozhevnikov@usu.ru

Keywords Stars: individual: FBS 1220 + 753 · Novae, cataclysmic variables · Subdwarfs · Stars: variables: δ Scuti · Stars: oscillations

1 Introduction

Cataclysmic variables (CVs) are interacting binaries that consist of a white dwarf primary accreting matter from a low mass secondary filling its Roche lobe. The path that the transferred matter takes depends strongly on the magnetic field of the white dwarf. A bright accretion disk forms in non-magnetic systems, while matter swirling along field lines releases energy in their magnetic counterparts. Because CVs are interacting binary systems, their emission from the X-rays to the infrared is generally totally dominated by the release of the gravitational energy of the accreted matter in a disk or an accretion column and not by the emission of the stellar components. In most cases CVs show emission line spectra. One of the most striking photometric characteristics common to all CVs are the variations with amplitudes from some hundredth of a magnitude up to one magnitude which have time scales ranging from seconds to a few dozen minutes, where higher amplitudes of variability occur at lower frequencies. This phenomenon is called flickering.

The First Byurakan Survey (FBS) was the first systematic objective prism survey of the extragalactic sky. Although the FBS was conducted originally to search for galaxies with UV-excess, the huge amount of spectral information contained in the plates allowed the development of several other projects based on the FBS, the most important being the discovery and investigation of blue stellar objects. The nature of many of them is still not clear (Mickaelian 2008). The object FBS 1220+753 (hereafter FBS1220) was selected from

the FBS as a blue stellar object with an emission line spectrum and was recognised as a CV (Abramyan and Mikaelyan 1995).

From the catalogue and atlas of CVs by Downes et al. (1997), Liu et al. (1999a) selected 55 CVs, which either did not have any published quiescent spectrum or had a reference spectrum that is only described, to obtain CCD spectrophotometric observations with the goal to confirm or disprove their CV nature because the lack of a published spectrum can leave their classification as CVs in doubt. FBS1220 was also included in this program. Liu et al. (1999b) obtained the spectrum of FBS1220, which turned out similar to that of a late-B to early-A type star without any trace of emission. But the high galactic latitude of FBS1220 (42°) excludes the possibility of its being a normal main sequence star. They therefore concluded that either the object was exactly in outburst (or has optically thick disk seen face-on) or this star does not appear to be a CV. In addition, the spectrum showed the presence of sharp NaD absorption, which could be expected to be enhanced by circumstellar (or interstellar) components, although the galactic latitude of this star is 42°. As a result, FBS1220 was reckoned among suspected CVs. However, even in outburst, discs cannot have spectra fully consistent with spectra of stars. Therefore, Downes et al. (2006) leave only two possibilities: either the object is not a CV, or is mis-identified (there is no chart published by Abramyan and Mikaelyan).

We decided to conduct photometric observations of FBS1220 with the goal to detect the flickering, which is inherent in all CVs, and thus it might confirm the membership of this star in the CV class. But, instead, we found a coherent oscillation with a period of 1.07 h. This oscillation was clearly visible directly in the light curve. To completely disclose its properties, we performed extensive photometric observations FBS1220. In this paper we present results of all our observations, spanning a total duration of 160 h within 28 nights.

2 Observations

In observations of CVs we use a multi-channel photometer with photomultiplier tubes that allows us to make continuous brightness measurements of two stars and the sky background. Such observations make it possible to obtain evenly spaced data. Then, in cases of smooth signals, classical methods of analysis such as the Fourier transform turn out optimal in comparison with numerous methods appropriated to unevenly spaced data (e.g. Lomb–Scargle periodogram) (Schwarzenberg-Czerny 1998).

FBS1220 was observed in 2010 February–March over 12 nights, in 2011 March–May over 13 nights and in 2012 February over 3 nights using the 70-cm telescope at Kourovka observatory, Ural Federal University. A journal of the observations is given in Table 1. The programme and comparison stars were observed through 16-arcsec diaphragms and the sky background was observed through a 30-arcsec diaphragm. The comparison star is USNO-A2.0 1575-03250646. It has $\alpha = 12^h22^m6\overset{s}{.}23$, $\delta = +74°58'14\overset{''}{.}4$ and $B = 14.7$ mag. Data were collected at 8-s sampling intervals in white light (approximately 300–800 nm), employing a PC-based data–acquisition system. We used the CCD guiding system, which enables precise centring of the two stars in the diaphragms to be maintained automatically. This improves the accuracy of brightness measurements and facilitates the acquisition of long continuous light curves. The design of the photometer and its noise analysis are described in Kozhevnikov and Zakharova (2000).

We obtained differences of magnitudes of the programme and comparison stars taking into account the differences in light sensitivity between the various channels. Because the angular separation between the programme and comparison

Table 1 Journal of the observations

Date (UT)	HJD start (−245 5000)	Length (h)
2010 Feb 8	236.371179	5.1
2010 Feb 9	237.144884	10.5
2010 Feb 11	239.119334	1.7
2010 Feb 18	246.125772	9.1
2010 Feb 20	248.142841	9.9
2010 Feb 21	249.147958	8.3
2010 Feb 22	250.139955	9.9
2010 Mar 6	262.268016	6.0
2010 Mar 17	273.354291	1.8
2010 Mar 18	274.168232	7.6
2010 Mar 20	276.184895	6.8
2010 Mar 23	279.259376	5.1
2011 Mar 28	649.242592	5.2
2011 Mar 30	651.223229	4.9
2011 Apr 1	653.197951	6.9
2011 Apr 4	656.341982	3.3
2011 Apr 9	661.207455	5.3
2011 Apr 25	677.238121	4.6
2011 Apr 27	679.248190	3.9
2011 Apr 28	680.282222	3.2
2011 Apr 29	681.279370	3.1
2011 May 4	686.260621	3.4
2011 May 5	687.260788	3.4
2011 May 6	688.269334	3.0
2011 May 7	689.275317	2.8
2012 Feb 19	977.194419	8.8
2012 Feb 20	978.129571	9.9
2012 Feb 21	979.133233	8.3

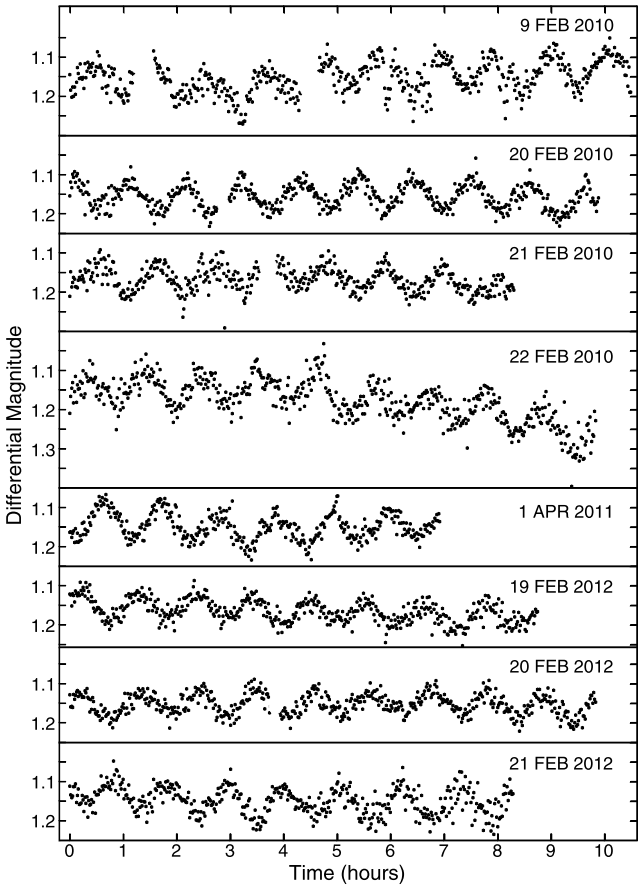

Fig. 1 Longest differential light curves of FBS 1220 + 753

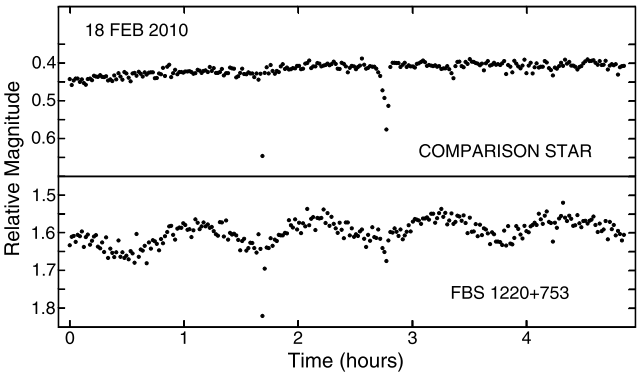

Fig. 2 Visible light curves of FBS 1220 + 753 and the comparison star that were obtained during a clear night. They show that the detected oscillation belongs to FBS 1220 + 753 and not to the comparison star

stars is small, the differential magnitudes were corrected for first-order atmospheric extinction and for other unfavourable atmospheric effects (unstable atmospheric transparency, light absorption by thin clouds etc.). According to the mean counts, the photon noise (rms) of the differential light curves is in the range 0.04–0.08 mag (a time resolution of 8 s). The actual rms noise also includes atmospheric scintillations and the motion of the star images in the diaphragms. We estimate that these noise components equal approximately 5 mmag each. They are relatively small and give no appreciable additions to the total noise. Figure 1 presents the longest differential light curves of FBS1220, with magnitudes averaged over 64-s time intervals. The white-noise component of these light curves is in the range 0.014–0.028 mag. Besides the white-noise components, each photometric system usually exhibits the $1/f$-noise component, which decreases the precision at frequencies below approximately 1 mHz (e.g. Young et al. 1991). As the noise analysis shows (Kozhevnikov and Zakharova 2000), in our photometer the $1/f$-noise component can reach 1.5–2.0 mmag at lowest frequencies in amplitude spectra calculated from individual light curves.

3 Analysis and results

As seen in Fig. 1, the differential light curves of FBS1220 show an oscillation. Because we perform differential photometry, in some cases it may be difficult to decide which of two stars shows oscillations. In the case of observations of FBS1220 this is simple task. The detected oscillation has relatively large amplitude and is easily visible not only in differential light curves but also in some light curves calculated directly from the counts of FBS1220 independently of the comparison star. Figure 2 presents two visible light curves of the comparison star and FBS1220 that were obtained in favourable atmospheric conditions. They leave no doubts that the detected oscillation belongs to FBS1220.

The light curves presented in Fig. 1 are not typical of CVs because they show no obvious flickering, which is usually visible as chaotic brightness variations. To find out whether FBS1220 exhibits weak flickering, which may be detectable as a continuous rise of the power at low frequencies, we calculated the average power spectrum for 18 longest light curves with the aid of a fast Fourier transform (FFT) algorithm. Previously, low-frequency trends were removed from the light curves by subtraction of a second-order polynomial fit. This power spectrum is presented in Fig. 3. At lowest frequencies it shows a noise level of about 14 mmag^2. This corresponds to the amplitude of 5.3 mmag. This noise level exceeds the $1/f$-noise level obtained in the noise analysis of the photometer (Kozhevnikov and Zakharova 2000) only by 2.5–3.5 times. Unlike the observations used for the noise analysis, which were made using R filter, here we observed in white light and used smaller diaphragms. In addition, the stars were much fainter and the individual light curves were longer. Due to these differences, the $1/f$-noise component of the photometer can increase. Moreover, the power spectrum shows no slope at frequencies above 1 mHz, where the $1/f$-noise component of the photometer is absent. Hence, we have no reliable evidence of the flickering in FBS1220.

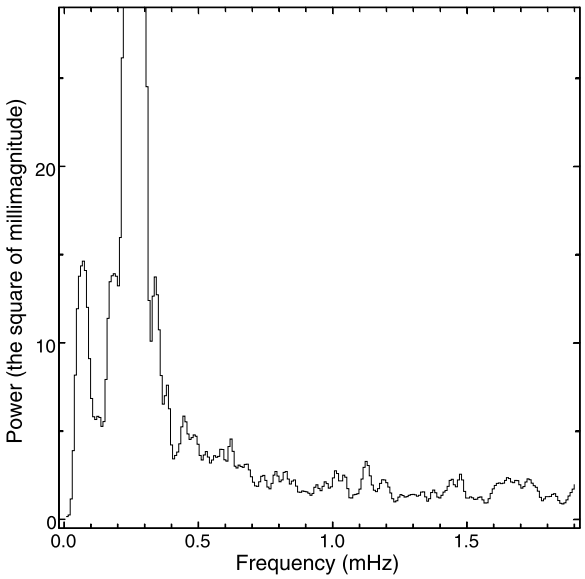

Fig. 3 Average power spectrum obtained from 18 longest individual light curves of FBS 1220 + 753. The huge peak corresponding to the detected oscillation is truncated

The individual light curves are too short and do not allow us to measure the period of the detected oscillation with high precision. Also it is well known that the frequency resolution of data depends on the observational coverage. Therefore, we analysed the data incorporated into common time series. To establish the stability of the oscillation period, first we analysed the data obtained in 2010 and 2011 separately. Two corresponding time series were composed from all the individual light curves from these data. Previously, low frequency trends were removed from the individual light curves by subtraction of a first- or second-order polynomial fit. The gaps due to daylight and poor weather in these time series were filled with zeroes. To improve the sampling of the power spectra, at the end these time series were supplemented with a considerable number of zeroes. Figures 4, 5 present the power spectra of these two common time series in the vicinity of the oscillation frequency that were calculated with the FFT algorithm. Both power spectra reveal distinct pictures closely resembling the window functions obtained from artificial time series consisting of sine waves and the gaps according to the observations (the upper

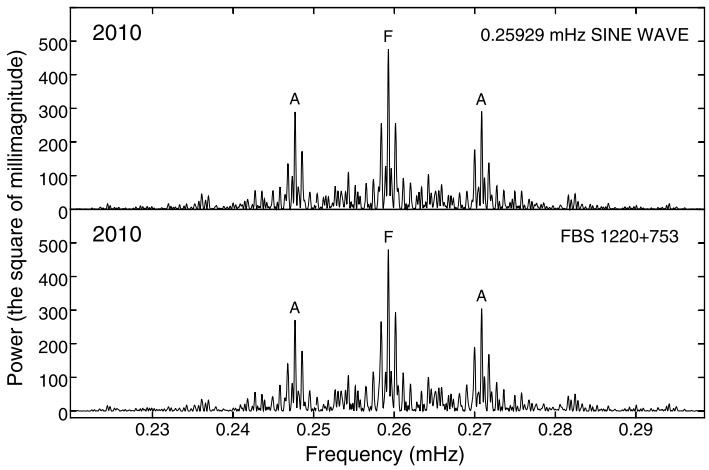

Fig. 4 Power spectra calculated for the data obtained in 2010 from FBS 1220 + 753 and for the artificial time series consisting of a sine wave and the gaps according to the observations. The principal peak is labelled with 'F' and the one-day aliases are labelled with 'A'

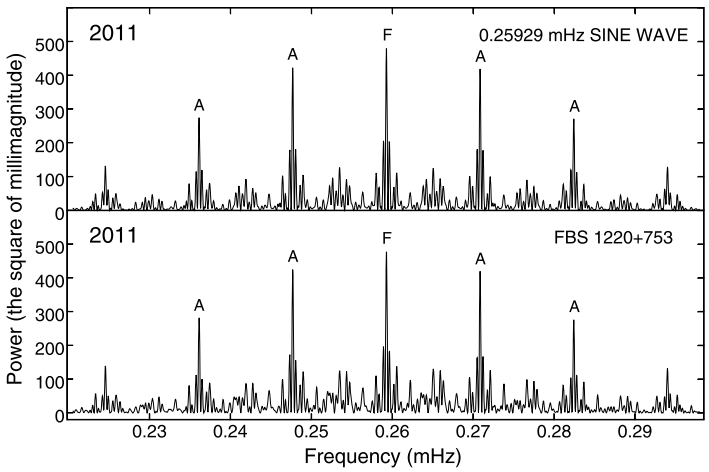

Fig. 5 Power spectra calculated for the data obtained in 2011 from FBS 1220 + 753 and for the artificial time series consisting of a sine wave and the gaps according to the observations. The principal peak is labelled with 'F' and the one-day aliases are labelled with 'A'

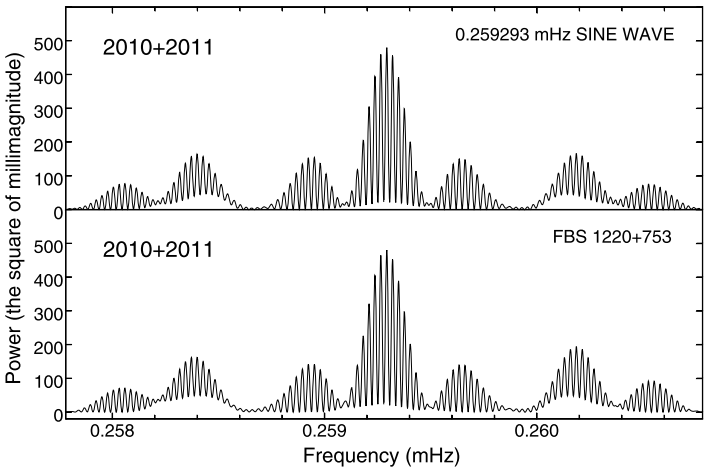

Fig. 6 Power spectra calculated for the data obtained in 2010 and in 2011 from FBS 1220 + 753 that were combined into the common time series and for the artificial time series consisting of a sine wave and the gaps according to the observations

frames of Figs. 4, 5). This proves the coherence of the observed oscillations during the corresponding time intervals.

Obviously, the highest accuracy of an oscillation period can be achieved from all data incorporated into common time series. However, in such a case the window function may be very complicated due to randomly distributed large gaps, and identification of principal peaks may be difficult. Really, the data obtained in 2012 are insufficient, and this does not allow correct identification of the principal peak in the power spectrum of all the data incorporated into the common time series, whereas the power spectrum of the common time series consisting of the data of 2010 and 2011 show a rather simple symmetric structure with the prominent principal peak. This power spectrum is shown in Fig. 6. Obviously, in this case we have no aliasing problem. The comparison of the oscillation periods obtained from the data of 2010 and 2011 and from this common time series also shows the absence of the aliasing problem. In detail this topic is described below. The close resemblance of the power spectrum from the data 2010 and 2011 and of the window function (the upper frame of Fig. 6) demonstrates that the oscillation is coherent during two years of observations.

A half-width of the peak at half maximum (HWHM) in the power spectrum is often accepted as an error of the period because this conforms to the frequency resolution. However, such a method does not allow for the noise of the data and in most cases gives an overestimated error. Schwarzenberg-Czerny (1991) showed that the 1σ confidence interval of the oscillation period is the width of the peak at the $p - N^2$ level, where p is the peak height and N^2 is the mean noise power level. Accordingly, the rms error (or σ) is half of this confidence interval. Recently we performed extensive photometric observations of the intermediate polar V515 And and made sure that the error obtained by such a way is a real rms error, i.e. it obeys a rule of 3σ (Kozhevnikov 2012). We used this method to evaluate the precision of the periods of the detected oscillation.

Table 2 The values and precisions of the oscillation period

Time interval	Period (h)	HWHM (h)	rms error (h)	Deviation
2010	1.071314	0.00044	0.000027	0.95σ
2011	1.071285	0.00042	0.000026	0.14σ
2010 + 2011	1.0712887	0.000029	0.0000013	–

As the mean noise level we took an average of two levels of the power spectrum in wide frequency intervals prior to and after the oscillation peak, where the power is unaffected by aliases. The precise maxima of the principal peaks were found by a Gaussian function fitted to the upper parts of the peaks. The results are presented in Table 2.

As follows from Table 2, the precision of the oscillation period from the data 2010 and 2011 taken as a whole is much higher than the precision of the oscillation periods from the data 2010 and 2011 taken separately. This period, namely 1.0712887 ± 0.0000013 h, can be considered absolutely precise with respect to two other periods. Therefore we can find the deviations of other periods and express them in units of their rms errors. The deviations are less than 1σ. This is shown in the fifth column of Table 2 and demonstrates that the obtained periods agree with each other. However, if we consider the nearest aliases as the principal peaks in the power spectrum (Fig. 6), then the deviations turn out in the range $3–5\sigma$. This proves the absence of the aliasing problem in the power spectrum of the data of 2010 and 2011 incorporated into the common time series.

As mentioned, to obtain the high sampling of the power spectra, we added a considerable number of zeroes at the end of the common time series. For the power spectrum of the data of 2010 and 2011, the sampling, which might allow us to measure the peak width, turned out extremely high, and this power spectrum consisted of 2^{25} points. To exclude any gross errors, which might be related with this giant number of points, we also calculated power spectra with the aid of

a sine wave fit to the light curves folded with trial frequencies and found the very close oscillation period, where the deviation was less than 0.3σ. In addition, we used the analysis of variance method (Schwarzenberg-Czerny 1989), and this also gave the very close period with the deviation of less than 0.2σ.

As follows from Table 2, the oscillation periods, which were obtained from the data of 2010 and 2011 separately, are very close, where the deviation is less than 0.8 of the summary rms error. This does not allow us to find the instability of the oscillation period. However, we can find the upper limit of the instability. The instability, dP/dt, turned out less than 3×10^{-9}. This upper limit of the instability seems rather large and does not allow us to make definite conclusions about the nature of the detected oscillation. Therefore, in 2012 we conducted additional photometric observations, which might detect the instability of the oscillation period or set the lesser limit of the instability. Although, as mentioned above, these observations are insufficiently prolonged and cannot be included into the common time series due to aliasing problem, they allow us to find the oscillation phase. Then through the change of the oscillation phase we might find the instability of the oscillation period. For that we must first find the oscillation ephemerides.

To obtain oscillation ephemerides, besides the oscillation period, it is necessary to know oscillation phases. A rather large noise level in the individual light curves does not allow us to find oscillation phases directly. Therefore, we found the oscillation phases from the folded light curves. We decided to obtain the initial phases from the data of 2010 and utilise the data of 2011 for verification. We used 20 phase bins for each folded light curve; therefore the time interval between adjacent points is 0.05 phases, and is equal to 1/20 of the oscillation period. Obviously, the first points of the folded light curves are at the distance of 0.025 phases from the very first observational point. Having the initial time of the observations (Table 1) and taking into account that the time of the very first observation point is late for 4 s compared to the initial time of the observations (8 s integration times in the photometer), we can find the initial time for the folded light curves. To precisely find the times of maxima and minima in the folded light curves, we used a Gaussian function fitted to 18–20 points around the maximum or minimum. Because the folded light curves were obtained from all the observations of 2010, it is true to refer the initial time of the ephemerides to the middle of the observations of 2010. Finally we obtained the following ephemerides:

$$HJD(max) = 245\,5257.83115(16) + 0.044\,637\,028(54)\,E \quad (1)$$

$$HJD(min) = 245\,5257.80883(11) + 0.044\,637\,028(54)\,E \quad (2)$$

Table 3 Verification of the oscillation ephemerides

Time interval	(O–C), maximum (s)	(O–C), minimum (s)
8 Feb–21 Feb 2010	-39 ± 24	-37 ± 17
22 Feb–23 Mar 2010	$+52 \pm 20$	$+52 \pm 17$
28 Mar–9 Apr 2011	$+6 \pm 45$	$+6 \pm 43$
25 Apr–7 May 2011	-28 ± 49	-30 ± 47
2011 all	-13 ± 46	-12 ± 45
2012 all	$+236 \pm 79$	$+236 \pm 78$

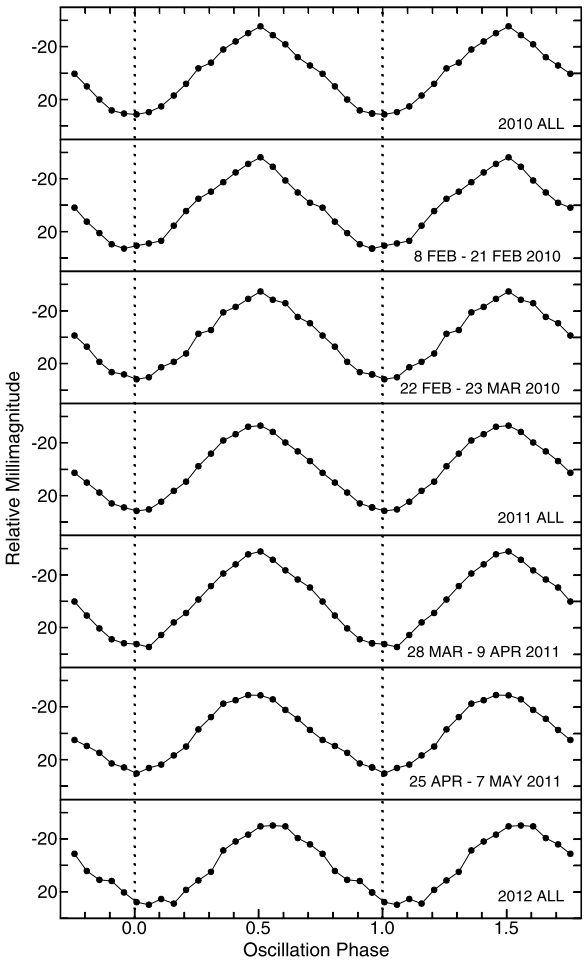

Fig. 7 Light curves of FBS 1220 + 753 folded with the oscillation period using the data subdivided into seven groups. The rms errors are less than the size of the points

To find changes of the oscillation phases during the observations, in addition to the folded light curves of the data obtained in 2010 and 2011, we subdivided the data into several smaller groups (see Table 3) and found the folded light curves for these groups. The folded light curve of the data obtained in 2012 was also found. The folded light curves are presented in Fig. 7. Table 3 gives observed minus calculated (O–C) values for the maxima and minima ob-

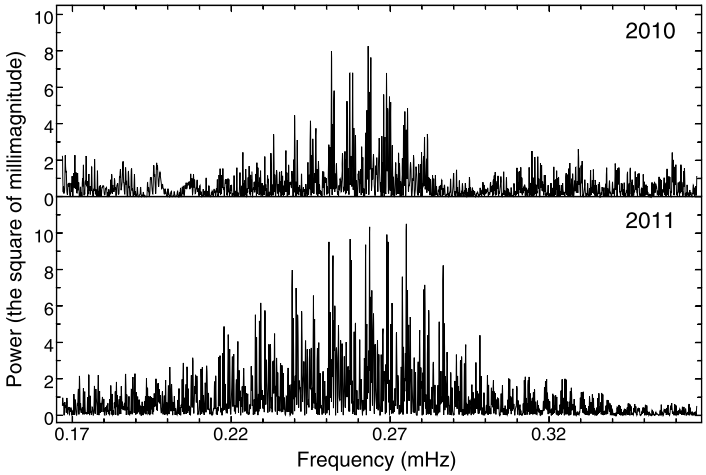

Fig. 8 Power spectra of the prewhitened data obtained in 2010 and in 2011 from FBS 1220 + 753

tained from these folded light curves by using the oscillation ephemerides. The rms errors are also given. They represent the summary rms errors from the errors of the initial and final maxima or minima and from the accumulated errors of the period. As seen, the (O–C) values for the data obtained in 2010 and 2011, including the smaller groups of these data, are small, where the deviations from the ephemerides do not exceed 3σ and are not systematic. This proves that the oscillation ephemerides are correct. Although the (O–C) values for the data obtained in 2012 seem large, the deviations from the ephemerides also do not exceed 3σ. Obviously, this is due to rather large accumulated errors. Therefore, we have no reason to declare the detection of the instability of the oscillation period in a time scale of years. Nonetheless, we can find the new upper limit of the period instability using the (O–C) values observed in 2012. To convert (O–C) into the period change, dP/dt, we used the following formula (Breger and Pamyatnykh 1998):

$$(\text{O–C}) = 0.5\frac{1}{p}\frac{dP}{dt}t^2. \tag{3}$$

According to this formula, the instability of the oscillation period, dP/dt, is to be less than $(4.1 \pm 1.4) \times 10^{-10}$.

As follows from the folded light curves (Fig. 7) and also from the power spectra, the oscillation semi-amplitude is stable and equal to 30 mmag. The pulse shape of the oscillation is very sinusoidal with slightly sharp maxima compared with minima. But this seems changeable from year to year.

The power spectrum obtained from the data of 2010 coincides in detail with the power spectrum of the artificial time series (Fig. 4). However, the power spectra of the data of 2011 and the corresponding artificial time series differ appreciably (Fig. 5). This suggests that additional oscillations with smaller amplitudes may be hidden in the complicated structures of the window functions. To find out this, we used the well-known method of subtraction of the larger oscillation from the data. The amplitudes and phases of the main oscillation were found from the folded light curves of the data of 2010 and 2011. Then we subtracted the corresponding sine waves from these data. The result is shown in Fig. 8. As seen, this procedure does not allow us to fully exclude the detected oscillation. The residual power spectra do also not allow us to detect an additional coherent oscillation because these power spectra do not correspond to the window functions (see the upper frames of Figs. 4, 5).

At higher frequencies (periods up to 16 s) the power spectra do not show additional coherent oscillations, which might be recognised due to typical forms resembling the window functions. The semi-amplitudes of the noise peaks turned out less than 4 mmag not far from the detected oscillation and less than 2 mmag at frequencies above 1 mHz. At very low frequencies the power spectra also do not show additional coherent oscillations. At very low frequencies, however, the noise peaks are much higher due to the increased $1/f$-noise of the photometer.

As seen in Fig. 8, after subtraction of the sine waves, the power spectra show a lot of small peaks. These residual peaks occupy the frequency range of the principal peak and one-day aliases of the detected oscillation. Hence, the residual variability of FBS1220 possesses certain coherence and is related with the detected oscillation. This also means that these pictures of the residual power spectra cannot be caused by the influence of the flickering (which is not detected) and photometric errors because the corresponding changes are incoherent. Therefore, these pictures must be caused by certain instability of the detected oscillation. We cannot explain such behaviour of the residual peaks only by the instability of the oscillation amplitude, because an oscillation with unstable amplitude can be excluded by subtraction of a sine wave with average amplitude. Hence, the oscillation instability is intrinsic and might be caused by small random changes of the oscillation phase in short time scales.

To find out what instability might cause the observed power spectra, we performed experiments with artificial

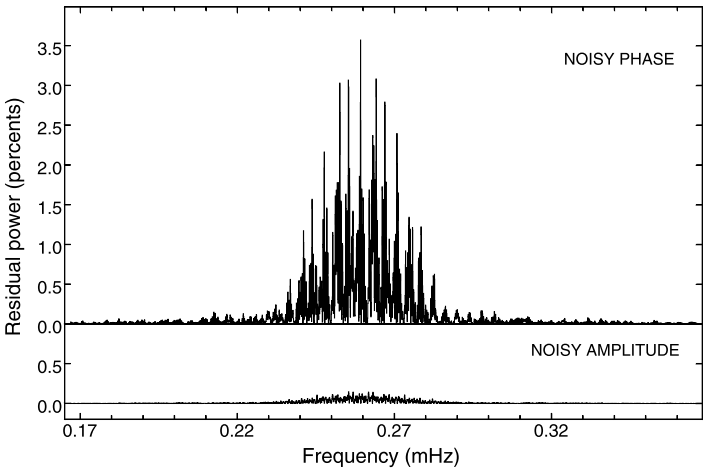

Fig. 9 Residual power spectra of two artificial time series after pewhitening. They demonstrate effects from noisy phase (rms of the changes is 5 % of the period) and from noisy amplitude (rms of the changes is 10 % of the average amplitude)

time series. For that we constructed several artificial time series consisting of a sine wave with a period of 1.07 h and with the gaps differing from the real gaps by small random time intervals. Obviously, these changes of the gap lengths simulate the instability of the oscillation phase. It turned out that the changes of the gap lengths with a standard deviation of less than 5 % of the period do not substantially affect the very power spectra. Nonetheless, these small changes produce humps of residual peaks visible after subtraction of the sine wave in the power spectra calculated with the real gaps. These humps look like the humps of residual peaks observed in the power spectra of the real data. The residual power spectrum of the artificial time series corresponding to the data of 2010 is shown in the upper frame of Fig. 9. It turned out that the changes of the gap lengths with a standard deviation of 5 % of the period produce the residual peaks with the height reaching 3.4–3.6 % of the oscillation power, whereas the changes of the gap lengths with a standard deviation of 2 % of the period produce the residual peaks with the height reaching only 0.4–0.5 %. In the real data the maximum height of the residual peaks is 1.7–2.2 % of the oscillation power. Hence, the random instability of the oscillation phase is in the range 2–5 % of the period.

To be confident that the changes of the oscillation phase are the only reason for the residual variability, we also performed experiments with artificial time series, in which the amplitude varies randomly. The residual power spectrum of the artificial time series corresponding to the data of 2010, in which the amplitude changes occur with a standard deviation of 10 % of the average amplitude, is shown in the lower frame of Fig. 9. As seen, even such large changes of the oscillation amplitude produce insignificant changes in the power spectrum. Such changes cannot be detected in the power spectrum of noisy data.

For sufficiently long individual light curves, it is possible to measure the random deviations of the oscillation phases by using cross-correlation functions calculated between these light curves and the sine waves which we used for prewhitening. Ten longest light curves obtained in 2010 seem suitable for this procedure. To find rms errors of the phase deviations, we performed numerous experiments with artificial time series. For that we constructed ten time series consisting of a sine wave with a period of 1.07 h, an amplitude of 0.03 and the initial phase corresponding to the initial time of the observations. The lengths of these time series were equal to the lengths of the real light curves. In addition, we constructed ten time series consisting of a sine wave with the same period and amplitude and with the phase displaced on 0.03. To these time series we added the white noise components with rms of 0.02, 0.03 and 0.04. Then we calculated cross-correlation functions between the time series consisting of the sine waves with the non-displaced and displaced phases. The phase displacements were found from the maxima of the cross-correlation functions, the precise positions of which were found by a Gaussian function fitted to 20 points around the maxima. Because the observed and true phase displacements are known, this makes it possible to find the rms errors. The phase differences (observed–pre-assigned) obtained from the experiments are presented in Table 4. In this table, in addition to the pre-assigned rms noise we give the correlation at maximum, which is related to this noise. It is useful for the direct estimation of the noise levels in the observed light curves.

As seen in Table 4, in the noise range 0.02–0.04, which we used for the experiments, the rms errors do not depend on the noise level. Moreover, the cross-correlation method gives appreciable errors even if the data do not contain the noise at all. To find out, what reasons give rise such a strange behaviour, we performed additional experiments with artificial time series. It turned out that the errors, which arise in the case when the noise in the data is absent, are related with the insufficient number of the oscillation cycles in the light curves and depend on the initial phase of the oscillation. In fact, these errors are systematic errors. However, because in the presence of the noise, it is difficult to find initial oscillation phases, we consider these errors as random errors.

Table 4 Errors found from artificial time series

Length (h)	Phase difference (s)			
	Noise 0.00 corr. 1.00	Noise 0.02 corr. 0.72	Noise 0.03 corr. 0.58	Noise 0.04 corr. 0.48
5.1	−12.2	−12.8	−10.4	−13.2
10.5	−4.1	−6.7	−2.6	−3.1
9.1	+4.4	−12.2	+3.7	+27.0
9.9	−2.8	−16.0	−13.3	+3.4
8.3	−4.6	+9.6	−22.8	−21.2
9.9	+4.8	+5.0	−2.5	+24.9
6.0	−24.6	−40.2	−21.5	+7.9
7.6	−14.4	−12.2	−9.4	−10.5
6.8	−5.6	−18.0	−15.8	−14.8
5.1	−7.8	−15.9	−37.3	+0.1
rms error	10.7	17.5	17.4	15.4

Table 5 Phase deviations in the light curves of 2010

Date (UT)	Length (h)	Corr. at maximum	Phase deviation (s)	Phase deviation (σ)
Feb 8	5.1	0.46	−73	4.3σ
Feb 9	10.5	0.40	+19	1.1σ
Feb 18	9.1	0.40	+2	0.1σ
Feb 20	9.9	0.52	−49	2.9σ
Feb 21	8.3	0.38	−21	1.2σ
Feb 22	9.9	0.40	+43	2.5σ
Mar 6	6.0	0.44	+124	7.3σ
Mar 18	7.6	0.52	+146	8.6σ
Mar 20	6.8	0.42	−93	5.5σ
Mar 23	5.1	0.37	−10	0.6σ

Moreover, they naturally give additions to the calculated rms errors because both the artificial time series and the real data contain signals with different initial phases. As seen in Table 4, the maximum rms error obtained from the experiments is equal to 17 s. We accept this error for the analysis of the real light curves. Note that the phase differences obtained in the experiments do not exceed this triple rms error in accordance with the rule of 3σ.

Table 5 presents results of measurements of phase deviations, which we obtained for ten longest light curves of 2010 by using the cross-correlation method. The precise positions of the maxima of the cross-correlation functions between the light curves and the sine wave used for prewhitening were found by a Gaussian function fitted to 20 points around the maxima. In the third column of Table 5 we give the correlation at maximum. This correlation is close to the correlation which corresponds to the noise of 0.04 in the artificial time series (see Table 4). Therefore, the estimation of the rms error made in the experiments seems true.

As seen in Table 5, in four cases the phase deviations significantly exceed 3σ and, hence, are real. In the extreme case the deviation reaches 8.6σ. The phase deviations show no systematic changes with time and seem random. The average absolute value of the phase deviations is equal to 1.5 % of the period. The largest phase deviation is equal to 3.8 % of the period. The phase deviations conform to the results obtained in the experiments with the random changes of the gap lengths. Moreover, these deviations averaged over corresponding time intervals are also approximately compatible with the phase deviations from the ephemerides in the folded light curves of 2010 (see Table 3). Thus, although the oscillation period is sufficiently stable in a time scale of years ($dP/dt < (4.1 \pm 1.4) \times 10^{-10}$), the detected oscillation reveals the phase instability at the level of a few per cent of the period in a time scale of days.

4 Discussion

We performed extensive photometric observations of FBS1220 during three years and clearly found the highly coherent oscillation with a period of 1.0712887 ± 0.0000013 h and with a stable semi-amplitude of 0.03 mag. We detected this oscillation for the first time. The pulse shape of the oscillation is very sinusoidal. In a time scale of years, the period of the oscillation is very stable ($dP/dt < (4.1 \pm 1.4) \times 10^{-10}$). In a time scale of days, however, this oscillation reveals the small instability of the oscillation phase, which is equal to a few per cent of the period.

As mentioned, FBS1220 was recognised as a CV in the course of the Byurakan spectral sky survey because this star showed the blue colour and emission line spectrum (Abramyan and Mikaelyan 1995). However, the spectrum obtained by Liu et al. (1999b) was similar to that of a late-B to early-A type star without any trace of emission. Because accretion discs in CVs cannot have spectra fully consistent with spectra of stars, two possibilities follow from the observation made by Liu et al.: either the object is not a CV, or is mis-identified (Downes et al. 2006).

Recently the first Byurakan spectral sky survey was digitised (Mickaelian 2008) and is available on The DFBS Web Portal (2012). In addition to scanned spectra of huge amount of objects, this survey contains images of plates with these spectra, which are also available. We checked the images of the plates, which contain the spectra of FBS1220, and made sure that the coordinates and chart of FBS1220 given by Downes et al. (1997, 2006) in the catalogue and atlas of CVs, which were used by Liu et al. and also by us, is true. Moreover, the spectrum obtained by Liu et al. corresponds to a blue star in accordance with the spectrum of FBS1220 in the Byurakan spectral sky survey whereas the spectra of nearby stars of similar brightness correspond to relatively red stars. So there is no incorrect identification.

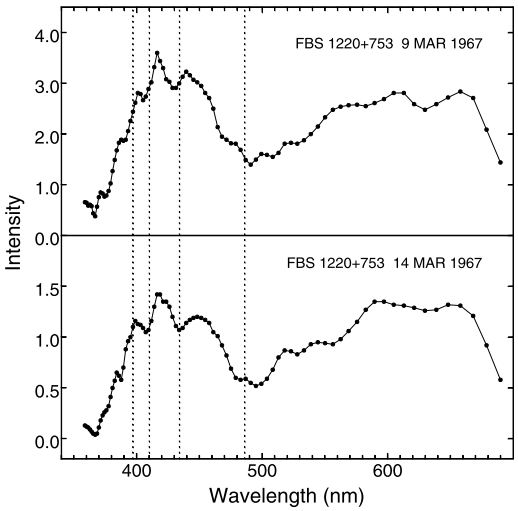

Fig. 10 Two DFBS spectra of FBS 1220 + 753. The *dotted lines* mark wavelengths of Hβ to Hϵ

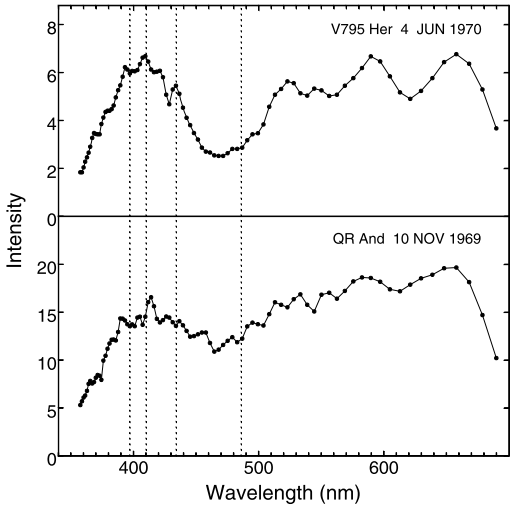

Fig. 11 DFBS spectra of the novalike variable V795 Her and supersoft X-ray source QR And, which are shown for comparison

In the digitised first Byurakan spectral sky survey (DFBS) we found three spectra of FBS1220. Two spectra, which have the best S/N ratio, are shown in Fig. 10. The DFBS spectra of two well-known objects are shown in Fig. 11 for comparison. These are the novalike variable V795 Her and supersoft X-ray source QR And. QR And is also reckoned among CVs (e.g. Ritter and Kolb 2003). As seen, the DFBS spectra have a rather low spectral resolution, where the resolution is improved in the blue spectral region. Obviously, such spectra can show only wide spectral lines. In the two spectra presented in Fig. 10 one can see at least one powerful emission line near 415 nm. This line is visible on approximately the same place and, therefore, cannot be caused by any defect of photoemulsion. Moreover, this line is perceptible directly by eye in the images of these spectra. Therefore it seems real. Although this line is not identifiable with hydrogen Balmer lines, this might be caused by the insufficient accuracy of the wavelength calibration. As seen in Fig. 11, two appreciable emission lines in the spectrum of V795 Her coincide with Hγ and Hδ, whereas the appreciable emission line in the spectrum of QR And near 415 nm does not coincide neither with Hγ nor with HeII (420 nm), which is more intense than Hγ and Hδ (e.g. Beuermann et al. 1995).

As follows from the comparison of Figs. 10 and 11, the emission line visible in the DFBS spectra of FBS1220 is not typical of CVs because it seems too wide. Such a wide line, if it is real, might probably denote an envelope resembling a planetary nebula. In the DFBS we found several spectra of planetary nebulas, which show similar and, in some cases, more wide and intense emission lines.

The DFBS spectra of FBS1220 were obtained when this star had B magnitudes of 14.8 and 15.0 (The DFBS Web Portal 2012). Liu et al. (1999b) obtained the spectrum of FBS1220 when it had a V magnitude of 15.2. To determine the brightness and colour of FBS1220, we performed photometry using one of the channels of the photometer as a simple one-channel photometer and two nearby stars with known B and V magnitudes as references (SA 5-506 and SA 5-507). We found $V = 15.34 \pm 0.03$ mag and $B - V = 0.25 \pm 0.04$ mag. As seen, during the observations spanning 45 years, FBS1220 underwent no significant brightness changes. Therefore, the disappearance of the emission line in the Liu et al. spectrum, which was visible in the DFBS spectra, cannot denote temporary cessation of mass transfer because in CVs the release of the gravitational energy of the accreted matter is dominant source of radiation. In addition, we found no obvious flickering in the light curves of FBS1220. Hence, we have no rigorous proofs that FBS1220 is a CV.

Although the spectrum obtained by Liu et al. was similar to that of a late-B to early-A type star, FBS1220 has a high galactic latitude (42°). This seemed to exclude the possibility of its being a normal main sequence star and did not allow Liu et al. to unconditionally abandon the CV hypothesis because such a star must be in the Galactic halo. Of course, in the Galactic halo the old blue main sequence stars must evolve away and turn into white dwarfs and red giants. Nonetheless, the Galactic halo is populated by blue stragglers, which are produced due to collisions between stars or mass transfer between the components of primordial short-period binaries (e.g. Perets and Fabrycky 2009). Moreover, the Galactic halo is also populated by metal-poor blue main sequence stars that are younger than the dominant population and were probably formed in external galaxies and accreted later on to our Milky Way (Jofré and Weiss 2011). Phenomenologically these stars are similar to blue stragglers. Although in the Galactic halo blue stragglers are relatively rare, the FBS blue stellar objects were selected

from the spectral survey of the extragalactic sky (i.e. excluding low galactic latitudes) and, therefore, the probability of such stars seems sufficiently high, especially among faint blue stellar objects.

Whereas FBS1220 can be a blue straggler, we can consider the possibility that this star is a SX Phe variable. The stars of this type, which are analogs of classical δ Sct variables of Population I, constitute significant portion of blue stragglers in the instability strip (e.g. Nemec et al. 1995), and their variability periods are compatible with the period observed in FBS1220. In addition, the colour of FBS1220 ($B - V = 0.25 \pm 0.04$ mag) is also compatible with δ Sct variables or SX Phe variables. FBS1220 has a galactic latitude of 42° and can undergo only weak interstellar reddening.

It is widely accepted that δ Sct stars and SX Phe stars pulsate in many oscillation modes. The shapes of the light curves, periods, and amplitudes of variable stars of these types usually vary greatly due to beating. Therefore, the main goal of our long observations of FBS1220 was to detect such instabilities, which might proof its belonging to pulsating variables. But both the period instability and the amplitude instability were not found. Additional oscillation frequencies were not found as well. Therefore, it seems unlikely that FBS1220 is a multiperiodic pulsating variable. Nonetheless, properties of the oscillations seen δ Sct variables and SX Phe variables are quite diverse (e.g. Breger 2009, 1993; Breger and Pamyatnykh 1998; Handler et al. 2000) and seem compatible even with the stable oscillation observed in FBS1220. Therefore, we cannot completely exclude possibility that FBS1220 is a pulsating variable of SX Phe type.

The revised and updated catalogue of the FBS blue stellar objects consist of 1101 objects. At present, the physical types of more than 2/3 of this sample are known due to additional investigations (Mickaelian 2008). Hot subdwarfs and white dwarfs comprise 80 % of these objects. It is quite reasonable to assume that hot subdwarfs and white dwarfs are also most numerous among the rest of objects with unknown nature. Whereas white dwarfs can be easily distinguishable from main sequence stars due to their spectra, it seems not true with respect to hot subdwarfs. Hot subdwarf B (sdB) stars show similar colours and spectral characteristics as main sequence stars of spectral type B, but are much less luminous. Compared to main sequence B stars the hydrogen Balmer lines in the spectra of sdB stars are stronger while the helium lines are much weaker (if present at all) for the colour (Geier et al. 2010). In moderate resolution spectra these differences can be inconspicuous by eye. Therefore, the spectrum of FBS1220 obtained by Liu et al. might be the spectrum of such an sdB star, but not the spectrum of a main sequence star. Then we can consider the possibility to account for the oscillation observed in FBS1220 by assuming that it is an sdB star.

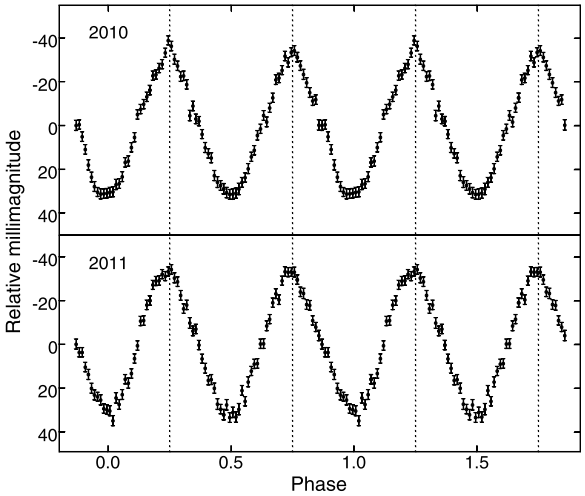

Fig. 12 Light curves of FBS 1220+753 folded with the doubled oscillation period. Each point is the average of about 460 (in 2010) and 300 (in 2011) individual brightness measurements. Note that the shapes of the adjacent oscillation cycles are remarkably different in the data of 2011

Whereas many sdB stars pulsate in several oscillation modes like δ Sct variables and SX Phe variables and, therefore, their light curves show unstable periods and amplitudes (e.g. Kilkenny 2002; Green et al. 2003), there are sdB stars, which show genuine periodic oscillations caused by eclipses, reflection effects or ellipsoidal variations. About two thirds of the sdB stats in the field are in close binaries with periods of less than 30 days, where secondary components can be main sequence stars or white dwarfs (Geier et al. 2010). A few sdB stars with ellipsoidal variations have very short orbital periods in the range 2.3–1.1 h. The corresponding oscillation periods, which are two times less, are compatible with the oscillation period observed in FBS1220. These sdB stars are IQ Cam (KPD 0422 + 5421) (Koen et al. 1998; Orosz and Wade 1999), V2214 Cyg (KPD 1930+2752) (Billères et al. 2000; Maxted et al. 2000), HE 0218–3437 (Koen et al. 2010) and CD–30 11223 (Geier et al. 2012; Vennes et al. 2012).

The light curves of FBS1220 show no eclipses. Therefore, two possibilities remain, i.e. reflection effect and ellipsoidal variations. Because ellipsoidal variations seen in the above-mentioned stars show different shapes of adjacent oscillation cycles, to find signs of ellipsoidal variations in FBS1220, we folded the light curves with the period, which was two times large than the oscillation period. The folded light curves are presented in Fig. 12. As seen, only in 2010 the adjacent oscillation cycles have similar shapes, whereas in 2011 the light curves show appreciable different depths of the adjacent minima, as may be due to ellipsoidal variations together with gravity darkening (Koen et al. 1998; Billères et al. 2000). But what is more remarkable, in 2011 the adjacent oscillation cycles show different shapes. The

odd oscillation cycles show a steep sinuous rise to maximum and a more gradual and nearly linear decline to minimum whereas the even oscillation cycles are symmetric with a nearly linear rise and decline (the lower frame of Fig. 12). To be confident that these differences are real, we also folded the light curves with a period, which was four times large than the oscillation period, and found similar picture.

Different shapes and different steepness of the rise and decline of the adjacent oscillation cycles are visible in the light curves of three sdB stars with ellipsoidal variations. These are IQ Cam (Fig. 3 in Koen et al. 1998), V2214 Cyg (Fig. 9 in Billères et al. 2000) and HE 0218–3437 (Fig. 5 in Koen et al. 2010). The similar behaviour of the shapes of the oscillation pulses in these three stars and in FBS1220 suggests that the oscillation seen in FBS1220 can be caused by ellipsoidal variations of a tidally distorted sdB star. Really, the similarity of the light curves of IQ Cam visible in Fig. 3 in Koen et al. (1998) and of the light curve of FBS1220 shown in the lower frame of Fig. 12 seems amazing. However, this similarity is observed only in 2011. The folded light curve FBS1220 obtained from the data of 2010 reveals the nearly identical shapes of the adjacent oscillation cycles (the upper frame of Fig. 12) and is different from IQ cam and other sdB stars with ellipsoidal variations. We cannot find plausible reasons for this changeability of the light curves. Thus, the nature of the oscillation seen in FBS1220 remains puzzling. To solve this puzzle, detailed spectroscopic observations are needed.

5 Conclusions

We performed extensive photometric observations of the suspected cataclysmic variable FBS1220 over 28 nights in 2010, 2011 and 2012.

1. The analysis of these data allowed us to clearly detect the highly coherent oscillation with a period of 1.0712887 ± 0.0000013 h and a stable semi-amplitude of about 0.03 mag.
2. The average pulse shape of the oscillation is very sinusoidal with somewhat sharper maxima compared with minima, but it is changeable from year to year.
3. In a time scale of years, the oscillation period is very stable, $dP/dt < (4.1 \pm 1.4) \times 10^{-10}$.
4. The careful analysis of the data shows that in a time scale of days the oscillation reveals the small phase instability with random phase changes within a few per cent of the oscillation period.
5. The light curves of FBS1220 show no obvious flickering. The significant brightness changes on large time intervals are also absent. Therefore, it is unlikely that FBS1220 is a cataclysmic variable.
6. The oscillation period and the colour of FBS1220 are compatible with oscillations seen in δ Sct variables and SX Phe variables. However, the high stability of the oscillation period and the absence of the appreciable changes of the oscillation amplitude during three years of the observations suggest that the oscillation cannot be caused by multiperiodic stellar pulsations.
7. The light curves of FBS1220 obtained in 2011 and folded with the doubled oscillation period reveals that the adjacent oscillation cycles show different shapes. This resembles the behaviour of the binary subdwarf–white dwarf systems, in which the variability is caused by ellipsoidal variations. However, the light curves of FBS1220 obtained in 2010 do not conform to such an interpretation. Detailed spectroscopic observations are needed to solve the puzzle of the oscillations seen in FBS1220.

Acknowledgements This work was partly supported by the Federal Goal-Oriented Program "Researches and elaborations on priority directions of development of a scientific-technological complex of Russia" (State contract 14.518.11. 7064). This work has made use of the Digitised First Byurakan Survey (DFBS), which is a joint project among the Byurakan Astrophysical Observatory (BAO, Armenia), "La Sapienza" Universita di Roma (Italy), and Cornell University (Ithaca, NY, USA).

References

Abramyan, G.V., Mikaelyan, A.M.: Astrophysics **38**, 108 (1995)
Beuermann, K., Reinsch, K., Barwig, H., et al.: Astron. Astrophys. **294**, L1 (1995)
Billères, M., Fontaine, G., Brassard, P.: Astrophys. J. **530**, 441 (2000)
Breger, M.: Astrophys. Space Sci. **210**, 173 (1993)
Breger, M.: In: Stellar Pulsation: Challenges for Theory and Observation. AIP Conf. Proc., vol. 1170, p. 410 (2009)
Breger, M., Pamyatnykh, A.A.: Astron. Astrophys. **332**, 958 (1998)
Downes, R.A., Webbink, R.F., Shara, M.M.: Publ. Astron. Soc. Pac. **109**, 345 (1997)
Downes, W., et al.: In: The Catalog and Atlas of Cataclysmic Variables. (2006). http://archive.stsci.edu/prepds/cvcat. Citet 30 Nov 2012
Geier, S., Heber, U., Podsiadlowski, Ph., et al.: Astron. Astrophys. **519**, A25 (2010)
Geier, S., Marsh, T.R., Dunlap, B.H., et al.: (2012). arXiv:1209.4740v1 [astro-ph.SR]
Green, E.M., Fontaine, G., Reed, M.D., et al.: Astrophys. J. **583**, 31 (2003)
Handler, G., Arentoft, T., Shobbrook, R.R., et al.: Mon. Not. R. Astron. Soc. **318**, 511 (2000)
Jofré, P., Weiss, A.: Astron. Astrophys. **533**, A59 (2011)
Kilkenny, D.: In: Aerts, C., Bedding, T.R., Christensen-Dalsgaard, J. (eds.) Radial and Nonradial Pulsations as Probes of Stellar Physics. Publ. Astron. Soc. Pac. Conf. Series, vol. 259, p. 356 (2002)
Koen, C., Kilkenny, D., Pretorius, M.L., Frew, D.J.: Mon. Not. R. Astron. Soc. **401**, 1850 (2010)
Koen, C., Orosz, J.A., Wade, R.A.: Mon. Not. R. Astron. Soc. **300**, 695 (1998)
Kozhevnikov, V.P.: Mon. Not. R. Astron. Soc. **422**, 1518 (2012)
Kozhevnikov, V.P., Zakharova, P.E.: In: Garzon, F., Eiroa, C., de Winter, D., Mahoney, T.J. (eds.) Disks, Planetesimals and Planets. Publ. Astron. Soc. Pac. Conf. Series, vol. 219, p. 381 (2000)

Liu, W., Hu, J.Y., Zhu, X.H., et al.: Astrophys. J. Suppl. Ser. **122**, 243 (1999a)
Liu, W., Hu, J.Y., Li, Z.Y., et al.: Astrophys. J. Suppl. Ser. **122**, 257 (1999b)
Maxted, P.F.L., Marsh, T.R., North, R.C.: Mon. Not. R. Astron. Soc. **317**, L41 (2000)
Mickaelian, A.M.: Astron. J. **136**, 946 (2008)
Nemec, J.M., Mateo, M., Burke, M., et al.: Astron. J. **110**, 1186 (1995)
Orosz, J.A., Wade, R.A.: Mon. Not. R. Astron. Soc. **310**, 773 (1999)
Perets, H.B., Fabrycky, D.C.: Astrophys. J. **697**, 1048 (2009)
Ritter, H., Kolb, U.: Astron. Astrophys. **404**, 301 (2003). Update RK-cat7.18, 2012
Schwarzenberg-Czerny, A.: Mon. Not. R. Astron. Soc. **241**, 153 (1989)
Schwarzenberg-Czerny, A.: Mon. Not. R. Astron. Soc. **253**, 198 (1991)
Schwarzenberg-Czerny, A.: Balt. Astron. **7**, 43 (1998)
The DFBS Web Portal (2012). http://byurakan.phys.uniroma1.it. Cited 20 Oct 2012
Vennes, S., Kawka, A., O'Toole, S.J., et al.: Astrophys. J. **759**, L25 (2012)
Young, A.T., Genet, R.M., Boyd, L.J., et al.: Publ. Astron. Soc. Pac. **103**, 221 (1991)